Active Closed-loop Control of Supersonic Impinging Jet Flows Using POD models*

Anuradha Annaswamy, Jae Jeen Choi, Debashis Sahoo,
Massachusetts Institute of Technology, Cambridge, Massachusetts, USA.

Farrukh S. Alvi, Huadong Lou
Florida A & M University and Florida State University, Tallahassee, Florida, USA.

Abstract

Fluid-flows exhibit pronounced acoustic resonances when a jet emerges from an orifice and impinges on an edge. One instance where such resonances, which are denoted as *edge-tones*, are produced is in a high speed jet from an STOVL aircraft nozzle impinging on the ground. Considerations of lift-loss, acoustic fatigue of nearby structures, and ground erosion mandate reliable and uniform reduction of these impingement tones during landing conditions. Recently, it has been shown that microjets located at the jet nozzle serve as effective actuators for the control of impingement tones. In this paper, a closed-loop control strategy for articulating the microjet pressure is suggested, in order to maintain a uniform, reliable, and optimal reduction of these tones over the entire range of operating conditions. This strategy is based on a POD-analysis of the pressure distribution along the azimuthal direction, where the microjet pressure distribution is matched to that of the dominant POD mode of the pressure. Preliminary experimental results from a STOVL supersonic jet facility at Mach 1.5 show that the mode-matched closed-loop strategy provides an additional 8-10 db reduction, compared to an open loop one, at the desired operating conditions.

1 Introduction

Several acoustic resonances have their origin in the instability of certain fluid motions. One of these motions is in the context of impinging high-speed jets. Experienced by STOVL aircraft while hovering in close proximity to the ground, impingement tones, which are discrete, high-amplitude acoustic tones, are produced due to feedback interactions between high speed jets emanating from the STOVL aircraft nozzle and the ground. These feedback interactions occur thus: Instability waves are generated by the acoustic excitation of the shear layer near the nozzle exit, which then convect down and evolve into spatially coherent structures. Upon impinging on the ground, the instability waves excite the waves of neutral acoustic modes of the jet, which in turn excite the shear layer at the nozzle exit, thereby closing the feedback-loop (see Figure 1 and [1]). The high-amplitude impingement tones are undesirable not only due to the associated high ambient noise, but also because of the accompanied highly unsteady pressure loads on the ground plane and on nearby surfaces. While the high noise levels can lead to structural fatigue of the aircraft surfaces in the vicinity of the nozzles, the high dynamic loads on the impingement surface can lead to an increased erosion of the landing surface as well as a dramatic lift-loss during hover.

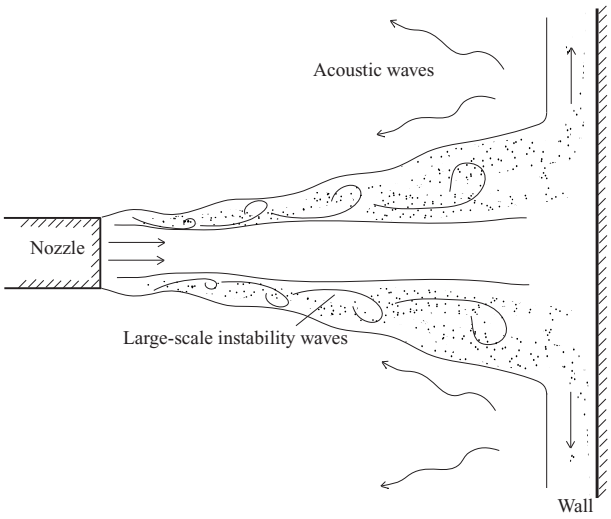

Figure 1: Schematic diagram of an impinging jet.

In an effort to reduce or eliminate these tones, several passive [2, 3, 4] and active control methods [5, 6, 7] have been attempted over the years to interrupt the feedback loop that is the primary cause of the impingement tones. Of these, the technique in [7] appears most promising from the point of view of efficiency, flexibility, and robustness. The method in [7] introduces microjets along the periphery of the nozzle exit which interrupt the shear-layer at its most receptive location thereby efficiently impacting the impingement tones. Due to their small size, these microjets can be optimally distributed along the circumference and can also

Proceedings of the 2002 IEEE CDC, Las Vegas, NV. This work is supported by an AFOSR grant, with Dr. J. Schmisseur as the program manager.

be introduced on-demand.

In [7], it is shown that an open-loop control strategy that employs the microjets is effective in suppressing the impingement tones. It was also observed in [7] that the amount of suppression is dependent to a large extent on the operating conditions. For example, it was observed in experimental studies that the amount of reduction that was achieved varied with the height of the lift-nozzle from the ground-plate as well as with the flow conditions. Since in practice, the operating conditions are expected to change drastically, a more attractive control strategy is one that employs feedback and has the ability to control the impingement tones over a large range of desired operating conditions. In this paper, we propose such a closed-loop control strategy for reducing the impingement tones.

In order to design a closed-loop control strategy, we adopt a model-based approach. A model of impingement tones, however, is quite difficult to derive due to the changing boundary conditions, compressibility effects, and the feedback interactions between acoustics and the shear-layer dynamics present in the problem. Since our primary goal is to model the impingement tone-dynamics and how they respond to microjet-control action at the nozzle, we will derive a reduced-order model that only captures these dominant dynamics and the effect of control. For this derivation, while tools based on stability theory [8] can be used to obtain some of the parameters such as the tonal frequencies, they are inadequate for deriving other model-details due to the complex features of the flow-field. Instead, we use the Principal Orthogonal Decomposition (POD) method and key measurements in the flow-field to derive the model. This model in turn is used to derive an appropriate closed-loop control strategy.

The Proper Orthogonal Decomposition (POD) is a tool used to extract the most energetic modes from a set of realizations from the underlying system [9]. These modes can be used as basis functions for Galerkin projections of the model in order to reduce the solution space being considered to the smallest linear subspace that is sufficient to describe the system. The decomposition is 'optimal' in that the energy contained in an N-ordered POD base is greater than any other N-ordered base in a mean-squared sense. Over the years, POD has been applied in several disciplines including stochastic processes, image processing, signal analysis, data compression, process identification and control in chemical engineering, and oceanography. In fluid mechanical systems, the POD technique has been applied in the analysis of coherent structures in turbulent flows and in obtaining reduced order models to describe the dominant characteristics of the phenomena. In this paper, our goal is to use the POD method to extract information about the mode shapes using pressure measurements in order to determine the control input strategy.

The paper begins with a reduced-order model of the impingement tones system that leads to the state-space representation in Section 2. In Section 3, the POD-based control strategy and the experimental results obtained in a high-speed STOVL facility at FSU are presented. A new method that recursively updates the POD modes online to accommodate their changes with operating conditions, is proposed in Section 4. Section 5 contains a summary of the paper.

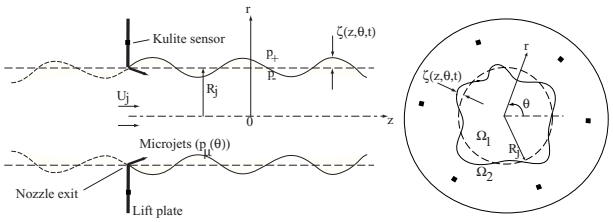

Figure 2: Vortex-sheet jet model for the impingement tones control problem. Location of microjets and pressure sensors also shown.

2 A Reduced-Order Model of Impingement Tones

The reduced-order model adopted for the control of impingement tones is based on the vortex-sheet jet model of [1]. Within a short distance ($\sim 0.01R_j$) downstream from the nozzle exit, the jet can be idealized as a uniform stream of velocity U_j and radius R_j bounded by a vortex sheet. Small-amplitude disturbances are superimposed on the vortex sheet (see Figure 2). This neglects the effect of the shock structure due to the microjet action and due to underdeveloped jet (if any) and the boundary effect of the ground. Let $p_+(r,\theta,z,t)$ and $p_-(r,\theta,z,t)$ be the pressures associated with the disturbances outside and inside the jet, denoted respectively by domains Ω_2 and Ω_1 where Ω_1 denotes jet-core which extends from $z=-\infty$ to $z=+\infty$, Ω_2 denotes the domain outside the jet-core and (r,θ,z) are the cylindrical coordinates. Also, let $\zeta(z,\theta,t)$ be the radial displacement of the vortex sheet. By starting from the linearized equation of motion of a compressible flow, it can be shown that the governing equations for the problem are:

$$\begin{aligned} \frac{1}{a_\infty^2}\frac{\partial^2 p_+}{\partial t^2} &= \nabla^2 p_+ \qquad (r\in\Omega_2) \\ \frac{1}{a_j^2}\left(\frac{\partial}{\partial t}+U_j\frac{\partial}{\partial z}\right)^2 p_- &= \nabla^2 p_- \qquad (r\in\Omega_1) \end{aligned} \quad (1)$$

where a_∞ and a_j are the speed of sound outside and inside the jet and U_j is the main jet speed.

The necessary boundary conditions that make the problem well-posed, are as follows.

C1. Equality condition at $r=R_j$:

$$p_+ = p_- \quad (2)$$

C2. Equality condition at $r=R_j, z\neq z_{nozzle}$:

$$\frac{\partial^2\zeta}{\partial t^2} = -\frac{1}{\rho_\infty}\frac{\partial p_+}{\partial r},$$

$$\left(\frac{\partial}{\partial t}+U_j\frac{\partial}{\partial z}\right)^2\zeta = -\frac{1}{\rho_j}\frac{\partial p_-}{\partial r} \quad (3)$$

C3. Introduction of microjets disturbs the vortex sheet, and its effect can be introduced as follows. At $r = R_j, z = z_{nozzle}$:

$$\left(\frac{\partial}{\partial t}+U_\mu(p_\mu)\frac{\partial}{\partial z}\right)^2\zeta = -\frac{1}{\rho_j}\frac{\partial p_+}{\partial r},$$
$$\left(\frac{\partial}{\partial t}+(U_j+U_\mu(p_\mu))\frac{\partial}{\partial z}\right)^2\zeta = -\frac{1}{\rho_j}\frac{\partial p_-}{\partial r} \quad (4)$$

where $p_\mu(\theta)$ is the microjet control pressure at the lift plate and $U_\mu(p_\mu)$ is the resulting microjet velocity.

C4. The zero normal flow condition on the lift plate is:

$$\frac{\partial p_+}{\partial n} = 0 \qquad (r \in \Omega_2, z = z_{nozzle}) \quad (5)$$

C5. From [1], for a stable solution of Equation (1) containing impingement tones, the Strouhal number $(2fR_j/U_j)$ range is limited to less than approximately 0.7 [†].

It may be noted that the pressure solution of [1] satisfies all the above boundary conditions except C3 and C4.

By separation of variables, we can write for the outer area Ω_2:

$$p_+(r,\theta,z,t) = \sum_{i=1}^{L} X_i(t)\Phi_i(r,\theta,z) \quad (6)$$

where X_i is the state variable, $\{\Phi_i\}$ is a set of orthonormal functions satisfying the boundary conditions (2-5) and hence can be viewed as the first L modes of the system. Clearly, $\{\Phi_i\}$ is a function of microjet pressure p_μ. Substituting in Equation (1), and taking inner product with respect to Φ_j, we get:

$$\ddot{X}_j(t) = a_\infty^2 \sum_{i=1}^{L} \left(\nabla^2\Phi_i, \Phi_j\right) X_i(t) \qquad j = 1,...,L \quad (7)$$

Since the modes are dependent upon p_μ, we can write Equation (7) in vector form as:

$$\dot{X}(t) = A(p_\mu)X(t) \quad (8)$$

3 The POD-based Closed-loop Control Strategy

The aim is to choose p_μ, the microjet pressure distribution such that $\|p_+(r,\theta,z,t)\|^2$ is minimized by making use of the pressure measurements made from the sensors placed on the upstream lift plate. In order to extract maximum possible information about the system, we adopt the Principal Decomposition Method (POD).

[†]In the current impingement tones problem, the Strouhal number was observed to be less than 0.63 in both microjets on- and off-cases.

3.1 The POD Algorithm

If $F(x,t)$ is a generalized zero-mean flow variable, then the POD method seeks to generate an approximation for F by using separation of variables as

$$\hat{F}(x,t) = \sum_{i=1}^{l} T_i(t)\phi_i(x) \quad (9)$$

where $T_i(t)$ is the ith temporal mode, $\phi_i(x)$ is the ith spatial mode, l is the number of modes chosen, and t and x are the temporal and spatial variables respectively. The POD method consists of finding ϕ_i such that the error $F(x,t) - \hat{F}(x,t)$ is minimized. This optimization problem can be stated as follows.

Denote $\{\phi_i(x)\}_{x=x_1,...,x_n} = \bar{\phi}_i \in \Re^n$. The POD method is the following optimization problem:

$$\begin{aligned} &\underset{\Psi}{\text{Min}}\ J_m(\bar{\phi}_1,...,\bar{\phi}_l) = \textstyle\sum_{j=1}^{m} \|Y_j - \sum_{k=1}^{l}(Y_j^T\bar{\phi}_k)\bar{\phi}_k\|^2 \\ &\text{subject to : } \bar{\phi}_i^T\bar{\phi}_j = \delta_{ij}, 1 \le i,j \le l, \Psi = [\bar{\phi}_1,...,\bar{\phi}_l] \end{aligned} \quad (10)$$

where $Y_j \in \Re^n$ is the vector of flow data F at time $t = t_j$. By definition [10], Ψ is a POD modal set if it is a solution to the optimization problem (10) for any value of $l < m$. The POD modal set can be obtained using the 'method of snapshots' [11, 12] as given below:

$$\phi_i(x_k) = \textstyle\sum_{j=1}^{m} \frac{\tilde{A}(j,i)Y(x_k,t_j)}{\sigma_i}, i = 1,...,l; k = 1,...,n \quad (11)$$

where $Y = \tilde{B}\Sigma\tilde{A}^T$, $\tilde{A}$ and $\tilde{B}$ are unitary matrices, and

$$\Sigma = \begin{bmatrix} \sigma_1 & & & \\ & \sigma_2 & & \\ & & \ddots & \\ & & & \sigma_l \end{bmatrix}, \sigma_1 \ge \sigma_2 \ge \cdots \ge \sigma_l.$$

The eigenvalues corresponding to the POD modes are the squares of the singular values $\{\sigma_1 \ge \sigma_2 \ge \cdots \ge \sigma_l\}$, and represent the energy content of the modes. In the context of the current problem, we note that Φ_i's in Equation (6) are the POD modes of the entire impinging flow field.

3.2 The Control Strategy

It can be seen from Equation (6) that in order to find the POD modes of the system, the calculation of pressure at all flow points is needed. This is not feasible either experimentally or computationally due to obvious constraints. However, our main goal is to model the impingement tones and it is worth noting that the key ingredients that contribute to their formation such as the initiation of the shear layer instability waves and their interaction with the acoustic waves appear to be localized at the jet nozzle. Therefore we derive the impingement tones model by focussing only on the POD of the pressure field close to the nozzle. That is, we derive the control strategy using the expansion:

$$p_+(r = R_s, \theta, z = z_{nozzle}, t) \stackrel{\Delta}{=} p(\theta,t) = \sum_{i=1}^{l} T_i(t)\phi_i(\theta) \quad (12)$$

where R_s is the radial position of the sensors on the lift plate. Note that ϕ_i's in Equation (12) are, quite likely, a subset of Φ_i's in Equation (6) which are the modes of the entire flow field. The state space equation corresponding to these reduced set of modes are given by:

$$\ddot{T}_j(t) = a_\infty^2 \sum_{i=1}^{l} \left(\nabla^2 \phi_i, \phi_j\right) T_i(t) \qquad j = 1, ..., l \qquad (13)$$

with the inner product suitably defined. In vector form, this becomes:

$$\dot{T}(t) = \breve{A}(p_\mu) T(t) \qquad (14)$$

Once the mode shapes are determined, we simply choose the control strategy as:

$$p_\mu(\theta) = k\phi_1(\theta) \qquad (15)$$

where ϕ_1 is the most energetic mode in Equation (12) and k is a calibration gain. The complete closed-loop procedure therefore consists of collecting pressure measurements $p(\theta, t)$, expanding them using POD modes as in Equation (9), determining the dominant mode ϕ_1, and matching the control input – which is the microjet pressure distribution along the nozzle – to this dominant mode as in Equation (15).

Remark 1: In order to guarantee that the closed-loop control leads to a uniform reduction of the impingement tones, we note that $\breve{A}(k\phi_1(\theta))$ must have stable eigen-values at desired locations. While an analytical derivation of the conditions under which this can occur is beyond the scope of this paper, as demonstrated in Section 3.3, this is indeed what occurs in the experimental investigations.

Remark 2: The closed-loop control approach used here is distinctly different from the traditional feedback control paradigm where the control input is typically required to be modulated at the natural frequencies of the system. The latter, in turn, mandates that the external actuator have the necessary bandwidth for operating at the natural frequencies. In the problem under consideration, the edge tones associated with the flow-field are typically a few kilohertz. Given the current valve technology, modulating the microjets at the system frequencies is a near impossibility. The approach presented above overcomes this hurdle by modulating the control input, p_μ, at a slow time-scale, so that it behaves like a parameter. If this control input is chosen judiciously, then even small and slow changes in this "parameter" can lead to large changes in the process dynamics, as is shown in the next section.

3.3 Experimental Results

The closed-loop control strategy described above was implemented at the STOVL supersonic jet facility of the Fluid Mechanics Research Laboratory, FSU (see [13] for details). Four banks of microjets were distributed around the nozzle exit, while pressure fluctuations were sensed using six *Kulite*^{TM} tranducers placed symmetrically around

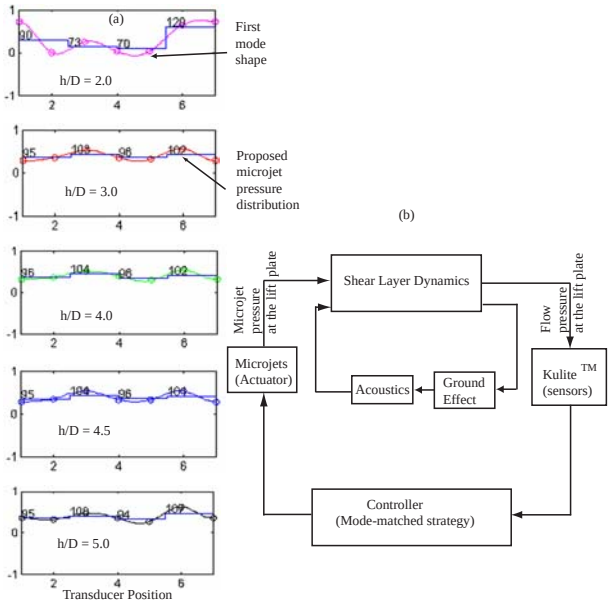

Figure 3: (a) The first mode shape and suggested microjet pressure distribution for each height. h is the height of the lift-plate from ground and D is the diameter of the lift-plate. (b) Block diagram of the closed-loop control program of impingement tones.

the nozzle periphery plate, at $r/d = 1.3$, from the nozzle centerline where d is the nozzle throat diameter. The control experiment was performed for a range of heights (of the nozzle above ground).

At each height, in addition to the mode-matched control, the active control strategy as given in [14] was also implemented. In the latter case, the spatial distribution of microjet pressure around the nozzle exit was kept uniform, and can be viewed as an open-loop control procedure. To ensure a fair comparison between the two control methods, the main nozzle was forced to operate under constant condition throughout the whole process. The calibration constant k in Equation (15) was chosen such that the minimum and maximum values of the POD mode over θ correspond to 70psi and 120psi, respectively, which ensured maximum effectiveness of the actuator. Figure 3(a) shows the shape of the first mode and the suggested microjet bank pressure distribution for several heights and Figure 3(b) shows a block diagram of the active closed-loop control method. Figure 4 shows the results for the closed loop control strategy, which indicates better performance throughout all operational conditions, with a large improvement at heights h/D = 4, 4.5 and 5. The reason for this increased pressure reduction can be attributed to the percentage of energy contained in the dominant mode, which is used in the control strategy. At heights 4 to 5, the energy content of the first mode is above 86%. In contrast, at heights 2 and 3, the energy level drops to about 50% and hence the corresponding improvement in the closed-loop strategy also drops to about half the db-value at heights 2 and 3 compared to at heights 4 and 5.

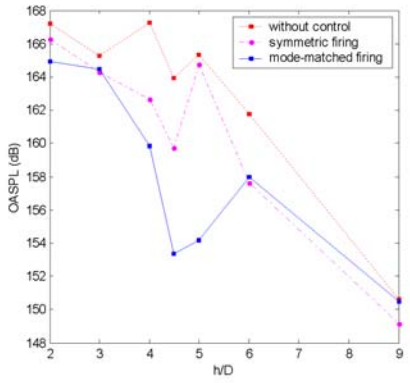

Figure 4: Overall sound pressure levels (OASPL) for different control (NPR=3.7).

4 RePOD-based Control in the Presence of On-line Perturbations

As Figure 3 indicates, the dominant POD mode shape changes with height of the nozzle from the ground. Since the closed-loop strategy in Equation (15) is dependent on the mode shape, as the STOVL aircraft approaches the ground, it requires the recomputation of the POD modes at each iteration of the control algorithm. By using the presently available techniques for computing the eigenfunctions, this requirement entails a significant amount of computational resources and time, especially since the set of plant realizations is large. Hence, POD cannot be readily used for an on-line implementation of an active closed-loop control strategy such as the one proposed here. More importantly, aside from computational issues, the iterative process of recomputing the POD modes with the current control input, and computing the control input using the updated POD modes, needs to be a stable one. In order to achieve a stable closed-loop system, we propose a new procedure that includes a Recursive Proper Orthogonal Decomposition (RePOD) algorithm (see [15] for details). Currently, work is being carried out to implement an autonomous active closed-loop control program to reduce the tones in the STOVL supersonic jet facility as the ground plate is moved upstream towards the nozzle, by using the RePOD technique. This technique is described below.

4.1 The RePOD Algorithm

Suppose we begin at time t_m, with $\bar{\phi}^{(m)}$, the POD solution to problem (10) corresponding to the flow data set $[Y_1,...,Y_m]$. Given a new measurement Y_{m+1} at time t_{m+1}, instead of minimizing J_{m+1}, we seek to minimize ΔJ, defined as

$$\begin{aligned} &\underset{\Psi}{\text{Min}}\ \Delta J(\bar{\phi}_1,...,\bar{\phi}_l) = \|Y_{m+1} - \textstyle\sum_{k=1}^{l}(Y_{m+1}^T\bar{\phi}_k)\bar{\phi}_k\|^2 \\ &\text{subject to : } \bar{\phi}_i^T\bar{\phi}_j = \delta_{ij}, 1 \le i,j \le l, \Psi = [\bar{\phi}_1,...,\bar{\phi}_l] \end{aligned} \tag{16}$$

The assumption is that with the addition of the new data set, the number of POD modes do not change.

Problem (16) can be solved as follows:

Step 1: Find $\bar{\phi}_1^{(m+1)}$ that minimizes $\Delta J^{(1)} = \|Y_{m+1} - (Y_{m+1}^T\bar{\phi}_1)\bar{\phi}_1\|^2$ over all $\bar{\phi}_1$ under the condition that $\phi_1^T\phi_1 = 1$.

Step i: Using the values of $\bar{\phi}_1^{(m+1)},\ldots,\bar{\phi}_{i-1}^{(m+1)}$, find $\bar{\phi}_i^{(m+1)}$ that minimizes over all $\bar{\phi}_i$, $\Delta J^{(i)} = \|Y_{m+1} - \sum_{k=1}^{i-1}(Y_{m+1}^T\bar{\phi}_k^{(m+1)})\bar{\phi}_k^{(m+1)} - (Y_{m+1}^T\bar{\phi}_i)\bar{\phi}_i\|^2$. Normalize $\bar{\phi}_i^{(m+1)}$. Continue for $i = 2,...,l$.

The minimization of $\Delta J^{(i)}$ in Step i can be carried out using gradient techniques as

$$\begin{aligned} \bar{\phi}_i^{(m+1)} &= \bar{\phi}_i^{(m)} - s\left.\frac{\partial \Delta J^{(i)}}{\partial \bar{\phi}_i}\right|_{\bar{\phi}_i=\bar{\phi}_i^{(m)}} \qquad (s>0) \\ &= \bar{\phi}_i^{(m)} + s\left(Y_{m+1} - \left(\sum_{k=1}^{j-1}\left(Y_{m+1}^T\bar{\phi}_k^{(m+1)}\right)\right.\right. \\ \bar{\phi}_k^{(m+1)} &+ \left.\left.\left(Y_{m+1}^T\bar{\phi}_i^{(m)}\right)\bar{\phi}_i^{(m)}\right)\right)\left(Y_{m+1}^T\bar{\phi}_i^{(m)}\right) \end{aligned} \tag{17}$$

Eq. 17 is the gist of the RePOD algorithm.

While the above algorithm does not guarantee orthogonality of the $\bar{\phi}_i^m$'s at each time t_m, as will be shown in the next section in the simulation examples, it leads to an orthonormal set of modes as $t \to \infty$. We also note that the recursive algorithm can be initiated by calculating the POD modes from the first m flow data sets. Under this initiation condition, the RePOD modes do not need to be orthogonal to be applied in any control problem involving POD analysis.

4.2 An Example

In order to evaluate the performance of the RePOD algorithm in Equation (17), we present a simple example in which the resident modes are assumed to change due to an arbitrary external perturbation.

We represent a flow variable F as a vector A, which is rotating in a plane in a 3-dimensional space, and abruptly transitions into another vector B whose plane of rotation is different from that of A (see Figure 5(a)). The POD modes of A and B are obviously distinct from each other while their number is equal to two in both cases. Moreover, the energy content of modes 1 and 2 are nearly equal to each other ($\sim$ 50%). The POD modes calculated using standard techniques [11] are also shown in Figure 5(b) for the two cases.

The RePOD algorithm in Equation (17) was then used, with the initial values of $\bar{\phi}_i$ as that obtained from a standard POD calculation using snapshots of vector A, and recursively updating them at each instant, using instantaneous values of the vector B. The results obtained are shown in Figure 5(c), which illustrate that the recursive technique is

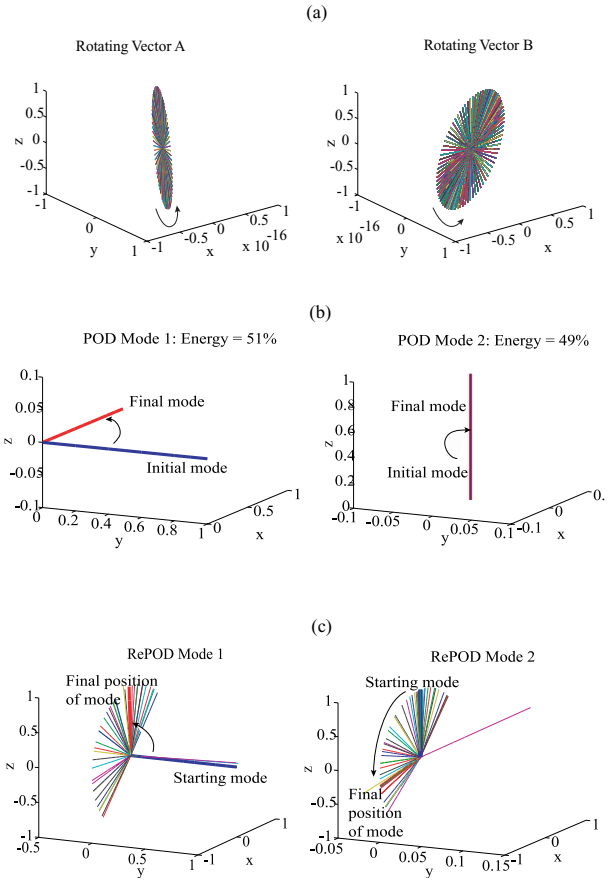

Figure 5: (a): Plane of rotation of the vectors A and B. (b): POD mode shapes of the rotating vectors A and B. The second mode of A and B are clearly the same. The energy levels of the modes are unchanged during the transition between A and B. (c): The RePOD mode shapes of the rotating vector B at the end of recursion. Calculation of mode shapes done using recursive technique with the following data: number of rotations = 3000, step size = 0.1, and angular speed = $\pi/4$ rad/s. The RePOD modes are in the $x-z$ plane, as desired.

able to capture the new mode shapes within an acceptable tolerance. Also, the RePOD modes are nearly orthogonal to each other ($\bar{\phi}_1^T \bar{\phi}_2 = -0.03$).

We repeated the above procedure for a different set of A and B, where A and B traverse a sector of a plane with the consequence that the POD modes, besides being distinct from each other, have an energy content of 95% in mode 1 and 5% in mode 2. The results obtained show that the change in modes is captured within an acceptable level of tolerance. The RePOD modes are once again closely orthogonal to each other ($\bar{\phi}_1^T \bar{\phi}_2 = -0.01$). Since number of snapshots used for the RePOD algorithm in this case is 10 times than that in the previous case, the resulting modes are more closely orthogonal to each other.

5 Summary

This paper proposes an innovative active closed-loop control strategy to suppress the impingement tones produced when the STOVL aircraft jet hits the ground. This strategy is based on a POD-analysis of the pressure distribution close to the nozzle exit along the azimuthal direction, and matches the microjet pressure distribution to that of the dominant POD mode of the pressure. Preliminary experimental results from a STOVL supersonic jet facility at Mach 1.5 show that the mode-matched closed-loop strategy provides an additional 8-10 db reduction, compared to an open loop one, at the desired operating conditions. Also, a new method that recursively updates the POD modes online to accommodate their changes with operating conditions, is proposed in the paper.

References

[1] C. K. W. Tam and K. K. Ahujae. Theoretical model of discrete tone generation by impinging jets. *J. Fluid Mech.*, 214:67–87, 1990.

[2] D.R. Glass. Effect of acoustic feedback on the spread and decay of supersonic jets. *AIAA Journal*, 6(6):1890–1897, 1968.

[3] L.J. Poldervaart, A.P.J. Wijnands, L.H.A.M. vanMoll, and E.J. van-Voorthuisen. Modes of vibration. *J. Fluid Mechanics*, 78:859–862, 1976.

[4] R. Elavarasan, A. Krothapalli, L. Venkatakrishnan, and L. Lourenco. Suppression of self-sustained oscillations in a supersonic impinging jet. *AIAA Journal (in press)*, 2002.

[5] M. Sheplak and E. F. Spina. Control of High-Speed Impinging-Jet Resonance. *AIAA Journal*, 32(8):1583–1588, 1994.

[6] C. Shih, F. S. Alvi, and D. Washington. Effects of Counterflow on the Aeroacoustic Properties of a Supersonic Jet. *Journal of Aircraft*, 36(2):451–457, 1999.

[7] F. S. Alvi, R. Elavarasan, C. Shih, G. Garg, and A. Krothapalli. "Control of Supersonic Impinging Jet Flows using Microjets". In *AIAA 2000-2236*, 2000.

[8] P. Huerre and P. A. Monkewitz. Absolute and Convective Instabilities in Free Shear Layers. *J. Fluid Mech.*, 159:151–168, 1985.

[9] P. Holmes, J. L. Lumley, and G. Berkooz. *Turbulence, coherent structures, dynamical systems and symmetry*. Cambridge University Press, 1996.

[10] S. Volkwein. "Proper Orthogonal Decomposition and Singular Value Decomposition". In *Technical Report, SFB-Preprint No. 153*, 1999.

[11] A. Newman. "Model Reduction via the Karhunen-Loève Expansion". In *Technical Research Report, T. R. 96-32 and 96-33*, Institute for Systems Research, University of Maryland, Maryland, USA, 1996.

[12] D. Tang, D. Kholodar, J.-N. Juang, and E. H. Dowell. System Identification and Proper Orthogonal Decomposition method applied to unsteady aerodynamics. *AIAA Journal*, 39, 2001.

[13] H. Lou, F. S. Alvi, C. Shih, J. Choi, and A. Annaswamy. "Active Control of Supersonic Impinging Jets: Flowfield Properties and Closed-loop Strategies". In *AIAA 2002-2728*, 2002.

[14] C. Shih, F. S. Alvi, H. Lou, G. Garg, and A. Krothapalli. "Adaptive Flow Control of Supersonic Impinging Jets". In *AIAA 2001-3027*, 2001.

[15] D. Sahoo, S. Park, D. Wee, A. Annaswamy, and A. F. Ghoniem. A Recursive Proper Orthogonal Decomposition Algorithm for Flow Control Problems. In *Technical report 0208, Adaptive Control Laboratory, MIT*, 2002.